Spectrochimica Acta Part A: Molecular and Biomolecular Spectroscopy 138 (2015) 763–773

Contents lists available at ScienceDirect

Spectrochimica Acta Part A: Molecular and Biomolecular Spectroscopy

journal homepage: www.elsevier.com/locate/saa

Temperature and high pressure effects on the structural features of catalytic nanocomposites oxides by Raman spectroscopy

Antonio N. da Silva [a,1], Raffael C.F. Pinto [a,1], Paulo T.C. Freire [a,1], Jose Alves L. Junior [a,1], Alcineia C. Oliveira [b,*], Josué M. Filho [a,1]

[a] Universidade Federal do Ceará, Campus do Pici-Bloco 922, Departamento de Física, Fortaleza, Ceará, Brazil
[b] Universidade Federal do Ceará, Campus do Pici-Bloco 940, Departamento de Química Analítica e Físico-Química, Fortaleza, Ceará, Brazil

HIGHLIGHTS

- Effect of temperature and pressure on nanostructured oxides by Raman spectroscopy.
- Phase transitions accelerated sintering of ZrO_2 and CeO_2 compared to TiO_2 and MnO_x.
- Rutile TiO_2 and t-ZrO_2 exhibited phase transition whereas CeO_2 and SnO_2 were stable.

GRAPHICAL ABSTRACT

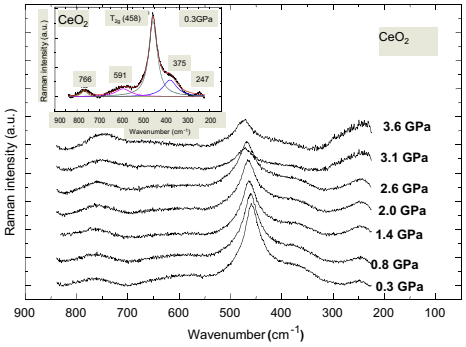

ARTICLE INFO

Article history:
Received 12 March 2014
Received in revised form 28 October 2014
Accepted 23 November 2014
Available online 29 November 2014

Keywords:
Raman spectroscopy
Phase transitions
Oxides
Nanostructures
Defects
Composite materials

ABSTRACT

Structural characterizations of nanostructured oxides were studied by X-ray diffraction (XRD), Raman and infrared spectroscopy. The oxides catalysts namely, SnO_2, ZrO_2, CeO_2, MnO_x, Al_2O_3 and TiO_2 were prepared by a nanocasting route and the effect of the temperature and pressure on the stability of the solids was evaluated. Raman spectra showed that ZrO_2 and TiO_2 exhibited phase transitions at moderate temperatures whereas CeO_2, SnO_2 and MnO_x had an effective creation of defects in their structures upon annealing at elevated temperatures. The results suggested also that the effect of the temperature on the particles growth is related to the type of oxide. In this regard, phase transition by up to 600 °C accelerated the sintering of ZrO_2 and CeO_2 grains compared to TiO_2, SnO_2 and MnO_x counterparts. Under hydrostatic pressures lower than 10 GPa, rutile TiO_2 and tetragonal ZrO_2 exhibited pressure induced phase transition whereas CeO_2 and SnO_2 were stable at pressures close to 15 GPa. The experiments revealed that the nanostructured SnO_2 oxide exhibited stable performance at relatively high temperatures without phase transition or sintering, being suitable to be used as catalysts in the range of temperature and pressure studied.

Introduction

Recent investigations have highlighted the ability of nanocomposites metal oxides to promote catalytic reactions [1,2]. Because of their versatile chemical, structural and electronic properties, the nanocomposites obtained by nanocasting method have

* Corresponding author. Tel./fax: +55 85 3366 99 82.
E-mail address: alcineia@ufc.br (A.C. Oliveira).
[1] Tel./fax: +55 85 3366 90 08.

http://dx.doi.org/10.1016/j.saa.2014.11.081
1386-1425/

attracted considerable interest in the fields of heterogeneous catalysis, electronics and magnetic materials [1–3].

Despite the large number of investigation on the origin of the structural properties ([1–5] and references therein), which have been published in the past, except a few studies carried out on co-precipitated materials, the influence of structural properties of the nanocasted oxides composites on the catalytic behavior has not been reported up to now. A systematic comprehension of the effect of temperature and pressure on the structure and texture of nanocasted SnO_2, TiO_2, CeO_2, ZrO_2, MnO_x and Al_2O_3 oxides is necessary, since it has been shown that both factors affect the catalytic properties of the solids [3].

In this context, manganese dioxide (MnO_2) can exist in several crystallographic forms, such as α-, β-,γ-, λ- and δ-types [6,7]. Since the MnO_6 octahedral units are linked in different ways such as in MnO_x, which is a mixture of Mn^{2+}, Mn^{3+} and Mn^{4+}, the structural flexibility of the oxides allows wide applications in catalysis such as oxidations and environmental reactions [7]. Alumina (Al_2O_3) has seven phases e.g., α-,γ-, χ-,θ-,κ-, ρ-, δ- and several hydrated forms, such as aluminum trihydroxide (bayerite) and monohydroxide (boehmite) possess a hexagonal crystalline structure. Alumina itself in α and γ forms is used as acid catalysts or catalytic support for epoxidation of toluene [8]. Ceria (CeO_2) is well known by its Ce^{4+}/Ce^{3+} redox cycles, which allows the oxygen-storage component properties in catalysts [1,3]. Titana (TiO_2) is widely applied in the optical thin film devices and photocatalysis, because of their desirable redox properties and its thermochemical stability in adverse environments [4,9]. It is noteworthy that zirconia (ZrO_2) interests are devoted to the acidic and basic reactions [10]. Tin dioxide namely cassiterite (SnO_2) is of great technological interest as n-type semiconductor with a large band gap catalysts, gas sensors, dye-based solar cells, transistors, electrode materials, electrochromic devices and as heat-reflecting filters [11]. The aim of the present work is to investigate the structure of nanocasted oxides catalysts through Raman measurements. Emphasis is given on the effect of the temperatures and pressure through the vibrational properties of the solids, since these intensive physical properties have strong influence on the catalytic behavior of the solids [12]. The use of well characterized nanocasted catalysts should provide a deep insight into the vibrational properties of the aforesaid oxides, which are of crucial importance for the development of promising catalytic applications.

Experimental

Synthesis of the solids

The CeO_2, TiO_2, SnO_2, MnO_x, ZrO_2 and Al_2O_3 monoxides catalysts were prepared by a nanocasting route using the hard mesoporous mold, as a sacrificial template. The preparation method to obtain CeO_2 and Al_2O_3 solids was modified from that of Abecassis-Wolfovich [1] and Lima [2], as follows: about 6 g of siliceous SBA-15 was used to prepare the SBA-15-supported cerium-oxide. The cerium $(NH_4)_2Ce(NO_3)_6$ methanolic solution was added dropwise through a peristaltic pump to a beaker containing 0.33 g of acetic acid, under stirring for 2 h. Then, additional amounts of acetic acid was added to every 10 g of mixed CeO_2 salt solution and then 1 g of SBA-15 silica was added to 10 mL of previous solution. Subsequently, propylene oxide was added to the suspension. The solid was separated by filtration and the SBA-15 containing hydrated cerium salt and the others reactants were aged for 16 h. The solid was washed, dried and calcined in air flow at 650 °C for 2 h to obtain the SBA-15-supported CeO_2 oxide. Finally, the solid was washed several times with water and exposed to 10 wt% HF solution under stirring for 1 h to remove partially the mesoporous silica to obtain the Ce solid. The Al nanocomposite was prepared by the same procedure, excepting the fact that $Al(NO_3)_3{\cdot}6H_2O$ was the aluminum precursor. SnO_2, MnO_x, ZrO_2 and TiO_2 nanocomposites were obtained using the $SnCl_4{\cdot}5H_2O$, $Mn(NO_3)_2{\cdot}6H_2O$, $ZrOCl_2{\cdot}8H_2O$ or $Ti(BuO)_4$ as metal sources. A 20 wt% ammonium hydroxide solution was added to the previous salts as the precipitant agent and nanopowder carbon, as previously described [2].

Characterizations

Powder XRD was carried out on a X-ray powder diffractometer Xpert MPD (Panalytical) using Cu Kα radiation (40 kV, 30 mA). The measurements were taken at wide angles. Crystallites average size of the solids was estimated from XRD patterns applying the Scherrer's equation. By using the planes, the particle sizes of SnO_2, MnO_x, ZrO_2 and TiO_2 nanocomposites were estimated; due to the broadening of the XRD lines however, crystallite sizes of CeO_2 and Al_2O_3 were not estimated. Table 1 summarizes the physicochemical properties of the solids obtained.

Mid and Far infrared spectroscopy measurements were carried out in a Bruker Vertex70® spectrometer coupled to a ATR instrument. The measurements were recorded in a 400–900 cm^{-1} range with a spectral resolution of 4 cm^{-1}.

Raman spectra of the solids were obtained on a T64000 Raman spectrometer (JobinYvon triple spectrometer) under ambient conditions, e.g. 23 °C. A 514.5 nm Ar laser was used as the exciting source on the sample surface with a power of 1 mW. The measurements were referenced to Si at 521 cm^{-1} with 16 data acquisitions in 120 s, with magnification of 100. In order to evaluate the effect of the temperature on the structural features of the solids, the measurements were performed by placing the solids in a cell allowing for *in situ* annealing and cooling measurements without solids manipulations. The solids were successively annealed at high temperatures (from 150 to 650 °C) in air and then the spectrum was collected. The annealing was repeated in steps of 150 °C until the completion of an eventual phase transformation, if it occurred. The samples were then cooled down to −23 °C. Crystallite sizes were estimated by Raman measurements for selected CeO_2 sample using the following equation:

$$\Gamma\ (\mathrm{cm}^{-1}) = 5.48 + 98.4/D_{calc}(\mathrm{Raman}) \quad (1)$$

where D_{calc} is the crystal size obtained from Raman spectrum by linear interpolation and standard deviations γ is the line width of the Raman modes [13].

High-pressure Raman measurements were performed using a Jobin Yvon spectrometer equipped with a N_2-cooled CCD system. The 514.5 nm line of an Argon ion laser was used as excitation source. An Olympus microscope lens with a focal distance f = 20.5 mm and a numeric aperture of NA = 0.35 was used to focus the laser on the sample surface and the slits were set for a resolution of 2 cm^{-1}. High-pressure Raman experiments were performed at room temperature by using a gasketed high-pressure Diamond Anvil Cell (DAC). Pressure was calibrated using the shifts of the

Table 1
Crystallographic parameters and BET surface area of the solids.

Solid	DRX phases[a]	Particle size [a](nm)	Textural properties[b]	
			Sg ($m^2\ g^{-1}$)	*Vp* ($cm^3\ g^{-1}$)
CeO_2	CeO_2	10.5	260	0.80
MnO_x	MnO_2 Mn_2O_3	24.3	201	0.58
Al_2O_3	γ-Al_2O_3	–	124	0.37
TiO_2	TiO_2	–	103	0.22
ZrO_2	ZrO_2	28	93	0.23
SnO_2	SnO_2	–	86	0.15

[a] From XRD data.
[b] N_2 adsorption–desorption measurements.